

SCIENTIFIC REPORTS



OPEN

Long-lived water clusters in hydrophobic solvents investigated by standard NMR techniques

Kouki Oka¹, Toshimichi Shibue², Natsuhiko Sugimura², Yuki Watabe², Bjorn Winther-Jensen³ & Hiroyuki Nishide^{1,4}

Unusual physical characteristics of water can be easier explained and understood if properties of water clusters are revealed. Experimental investigation of water clusters has been reported by highly specialized equipment and/or harsh experimental conditions and has not determined the properties and the formation processes. In the current work, we used standard ¹H-NMR as a versatile and facile tool to quantitatively investigate water clusters in the liquid phase under ambient conditions. This approach allows collection of data regarding the formation, long lifetime, stability, and physical properties of water clusters, as a cubic octamer in the liquid phase.

The unusual physical characteristics of water, such as its high boiling/freezing point, the abnormal temperature dependency of its density, and ice nucleation for freezing, can be easier explained and understood if water exists as clusters rather than isotropic molecules. This has prompted intensive experimental and theoretical investigation of the structure and properties of water clusters^{1–20}. However, experimental studies of water cluster in gas-phase are reported by the need for highly specialized equipment and/or harsh experimental conditions^{3,5–7}. While these studies have been successful in detecting water clusters, they have not determined the properties of water clusters or directly and quantitatively measured the processes whereby they form and transform.

Frank *et al.* proposed the first idea that water molecules orient themselves preferentially around the hydrophobic benzene^{9,10}. There have been few experimental studies on water clusters in a hydrophobic solvent^{11–15}. Lange *et al.* analysed water in benzene by Fourier transform infrared (FT-IR) transmission/absorption and X-ray absorption spectroscopy¹¹. Thorsten *et al.* performed IR measurements of water-containing carbon tetrachloride and suggested a cluster-like structure of water¹². Nakahara and Wakai preliminarily suggested that the ¹H-NMR signals of water clusters in CCl₄, C₆D₆ and CDCl₃ shift from those of dissolved and bulk water¹⁵.

Here, we describe experimental characterization of water clusters by standard NMR spectroscopy under ambient conditions in hydrophobic solvents (benzene is a typical example). A metastable water cluster easily forms by cooling the hydrophobic solvents saturated with water. The samples exhibit an additional NMR signal assigned to water protons with strong hydrogen bonding (“water clusters”) separate from the signals of water dissolved in the hydrophobic solvent (“dissolved water”) and water aggregates (“bulk water”) ^{15,21}. The ¹H-NMR signal specifically related to water clusters allows both qualitative and quantitative characterization. In the current work, we found that there was only one type of water clusters to be generated in hydrophobic solvents. We also investigated thermodynamic properties, kinetics, and additional information of water clusters.

Results and Discussion

Slightly more water than the solubility limit (0.57% water volume) was added to benzene-d₆ in a sealed NMR tube at 298 K, and the tube was then warmed at 343 K to make the homogeneous sample solution fully saturated with dissolved water. The typical ¹H-NMR spectra before and after warming are shown in Fig. 1a,b, respectively, where the proton signals are assigned to bulk water and dissolved water. ¹H-NMR chemical shift at a higher magnetic field indicates that dissolved water exists as single molecules^{15,21}. The solution was then cooled to 298 K. The ¹H-NMR spectrum of the supersaturated solution contains an additional sharp signal at significantly

¹Department of Applied Chemistry, Waseda University, 3-4-1 Okubo, Shinjuku, Tokyo, 165-8555, Japan. ²Materials Characterization Central Laboratory, Waseda University, 3-4-1 Okubo, Shinjuku, Tokyo, 165-8555, Japan.

³Department of Advanced Science and Engineering, Waseda University, 3-4-1 Okubo, Shinjuku, Tokyo, 165-8555, Japan. ⁴Research Institute for Science and Engineering, Waseda University, 3-4-1 Okubo, Shinjuku, Tokyo, 165-8555, Japan. Correspondence and requests for materials should be addressed to T.S. (email: shib@waseda.jp) or H.N. (email: nishide@waseda.jp)

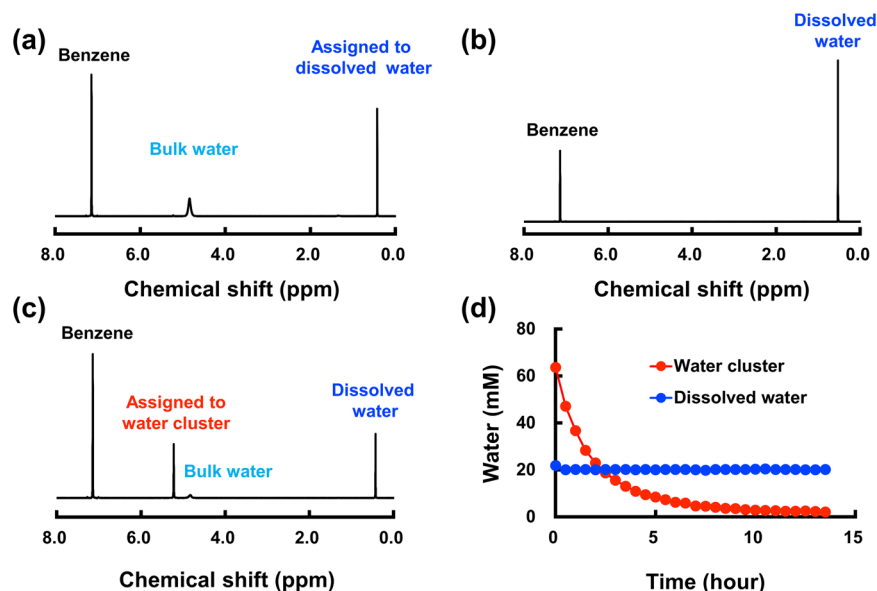


Figure 1. ^1H -NMR spectra of long-lived water clusters. (a) ^1H -NMR spectrum of benzene- d_6 mixed with a small amount of water (0.57% water volume content in benzene- d_6) at 298 K. (b) ^1H -NMR spectrum of water in benzene- d_6 kept at 343 K. (c) ^1H -NMR spectrum of water in benzene- d_6 solution cooled to 298 K. (d) Changes of the proton signal intensities assigned to the water cluster and dissolved water with time at 283 K. The residual proton signals of benzene in (a–c) are from residual benzene in the benzene- d_6 solvent.

lower magnetic field than that of trace bulk water (Fig. 1c). The proton signal with a very large chemical shift of 5.25 ppm suggests the presence of water with a very strong hydrogen-bonding structure, which we call a “water cluster”, compared with that of bulk water¹⁵. The additional sharp signal with the chemical shift of 5.25 ppm appears also through sonication of the same mixture of benzene- d_6 with a small amount of water (Supplementary Fig. S1b). We also measured D_2O concentration-dependent chemical shift of water clusters in Fig. S1c,d. These results validate that the observed peak is from a water entity. The dissolved water (single molecules) is stable and entropic favourable below the solubility limit. When the dissolved water becomes supersaturated, the single water molecules quickly and spontaneously form water clusters.

It should be noted that the instantaneous appearance of the ^1H -NMR signal is not observed for water mixtures of polar solvents, where the proton signal of dissolved water continuously shifts downfield with increasing water concentration (Supplementary Fig. S2a). The proton signal assigned to the water cluster is also observed for benzene derivatives, such as toluene and xylene (chemical shifts of 5.19 and 5.17 ppm, respectively, Supplementary Table S1), and even for other hydrophobic solvents, such as chloroform (Supplementary Fig. S2b). Appearance of a new very sharp proton signal of water with a large chemical shift is specific to water supersaturated in hydrophobic solvents. The solvent effect to the ^1H -NMR signals of water clusters at different solvent ratios are shown in Fig. S2c. This suggests that there is only one type of water cluster structures to be generated in hydrophobic solvents such as benzene, toluene, xylene, chlorobenzene, dichlorobenzene, trichlorobenzene, cyclohexane, carbon tetrachloride and chloroform.

As a control experiment, FT-IR spectroscopy was performed for the same sample solutions (Fig. 2). The IR absorption peaks assigned to dissolved water (and bulk water) are overlapped in a broad peak (probably ascribed to a water cluster). For the IR measurements under ambient conditions, it is not surprising that the absorption peak of bulk water (and also the water cluster) broadens because of dynamic hydrogen bonding, which will be discussed later.

Diffusion-ordered and nuclear Overhauser effect (DOSY and NOESY) spectroscopy and spin-lattice T_1 and spin-spin T_2 relaxation time measurement were performed to characterize the water clusters. DOSY spectroscopy gave diffusion coefficients for the protons ascribed to dissolved and bulk water of 5.0 and $2.3 \times 10^{-9} \text{ m}^2 \text{ s}^{-1}$ (Supplementary Fig. S3), respectively, which agree well with previously reported values^{22–24}. However, the diffusion coefficient of the water cluster ($0.5 \times 10^{-9} \text{ m}^2 \text{ s}^{-1}$) is surprisingly low (about 1/10 and 1/5 that of dissolved and bulk water, respectively). This means that the water molecules in the cluster have very restricted mobility. We showed the picture of the NMR tube (Fig. S1b inset) to show the good homogeneity of the sample. The good homogeneity indicating that the measured effect is not related to artefacts on the glass surface. The T_1 and T_2 measurement gave the correlation time T_C which characterized the interaction induced by molecular motions, and indicated that the protons in water clusters had a longer correlation time with the nearest neighbour water molecules than that in bulk water (Supplementary Table S2)¹⁴.

NOESY spectroscopy (Supplementary Fig. S4) shows proton exchange (a negative nuclear Overhauser effect) between the dissolved water and the water cluster, which means that both the dissolved water and the water cluster are solutes in benzene and coexist (are in equilibrium) with a mutual interaction. In addition, the chemical

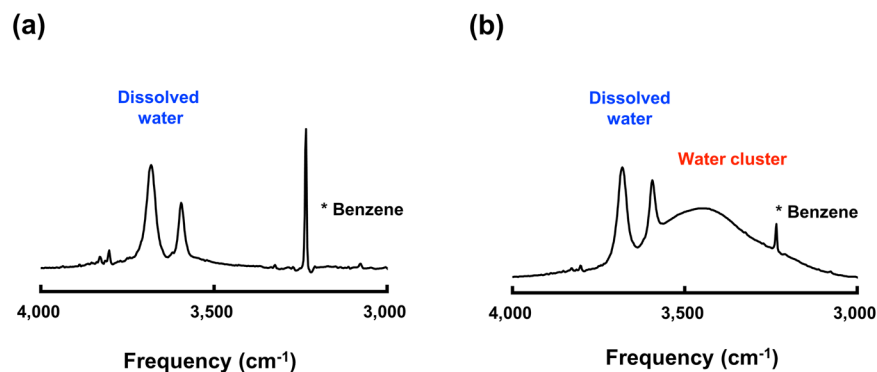


Figure 2. FT-IR spectra of water cluster and dissolved water. (a) FT-IR spectrum of benzene-d₆ mixed with a small amount of water (corresponding to Fig. 1b) at 298 K. (b) FT-IR spectrum of the water cluster and dissolved water in benzene-d₆ (corresponding to Fig. 1c) at 298 K. The absorption spectrum of benzene-d₆ was subtracted from each measured spectrum. The peaks are assigned to the symmetric (3594 cm⁻¹) and asymmetric (3691 cm⁻¹) vibration modes of water molecules, strongly tetrahedrally coordinated hydrogen bonding (3100–3400 cm⁻¹), and weak hydrogen bonding (3400–3700 cm⁻¹)¹³.

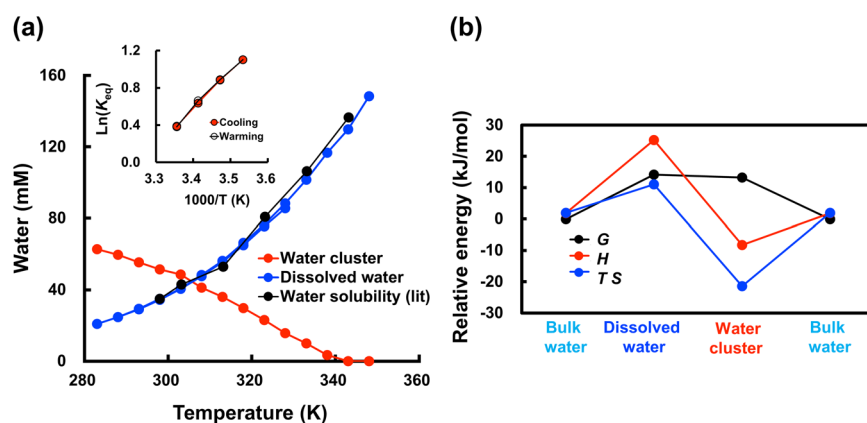


Figure 3. Thermodynamic properties of water clusters. (a) Formation of a water cluster by cooling a 0.57% water/benzene-d₆ solution from 323 to 283 K (5 K step). The concentrations of dissolved water and the water cluster in benzene-d₆ were normalized to the water concentration reported in the literature and handbook²⁵ at 298 K. Inset: van't Hoff plots for the equilibrium between the dissolved water and the water cluster (K_{eq} : apparent equilibrium constant). (b) H and S values for bulk water at 298 K were cited from ref.²⁶ which assumed values of zero at 273 K. The ΔH and ΔS values between bulk water and dissolved water in benzene were taken from ref.²⁷. The ΔH and ΔS values of the water cluster are from this work. The ΔG values were calculated using the classical equation $\Delta G = \Delta H - T\Delta S$.

exchange build-up curve by different mixing time indicates that the exchange rate between water clusters and dissolved water is faster than that of the bulk water and dissolved water.

The ¹H-NMR signal assigned to the water cluster slowly decreases with time (Fig. 1d), although the signal is still detectable after 3 days even at 298 K (Supplementary Fig. S5). The water cluster is in a metastable state, and the data measured within 15 min do not cause a significant difference (error <2%).

The temperature dependences of the NMR signal intensities assigned to dissolved water and the water cluster are shown in Supplementary Fig. S3a. The concentration of the water cluster increases with decreasing temperature accompanied by a quantitative and complementary decrease in the dissolved water amount, and the water cluster concentration reversibly decreases by increasing the temperature.

To investigate the equilibrium between dissolved water and the water cluster, the reversibility, or quasi-thermodynamical stability, of water cluster formation was analysed by the classical van't Hoff plot (Inset of Fig. 3a). The ΔH , ΔS , and ΔG values for water cluster formation from dissolved water were determined from the straight line in the van't Hoff plot to give the energy diagram (Fig. 3b). The large enthalpy gains for formation of the water cluster from dissolved water (about 34 kJ/mol) could be the driving force for cluster formation, which can be ascribed to formation of multiple hydrogen bonds. However, cluster formation is accompanied by a large entropy loss (about -110 J/mol K). This can be explained by cluster formation, or formation of a more ordered structure. ΔG to form the water cluster from dissolved water, which is the sum of the large enthalpy gain and entropy loss, is slightly negative, and the water cluster is a thermodynamically metastable state.

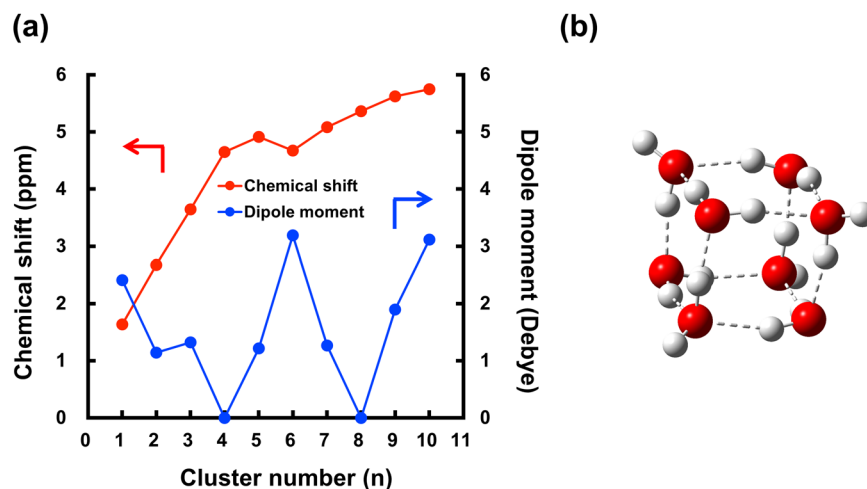


Figure 4. Calculated characteristics of water clusters. (a) Calculated chemical shifts (ppm) of the protons and dipole moments (Debye) of water clusters with different n . (b) Estimated D2d structure of a water octamer. The calculation of NMR chemical shifts and dipole moments were performed utilizing the second-order many-body perturbation theory and gauge-including atomic orbitals with integral equation formalism for the polarizable continuum model of the benzene solvent^{29,30}.

Transformation from the water cluster to bulk water has a negative ΔG value (Fig. 3b), and the water cluster is indeed finally converted to bulk water. An example of decay of the water cluster with time is shown in Fig. 1d. During a separate series of $^1\text{H-NMR}$ measurements, spinning of the sample tube in the instrument accelerates transformation of the water cluster to bulk water, where second-order kinetics is dominant. The temperature dependency of the decay rate in the Arrhenius plots gives an apparent activation energy of decay of 38 kJ/mol (Supplementary Fig. S6). The large activation energy of cluster decay supports that the water cluster is a metastable state.

The size-specific small water cluster number n has been discussed using the experimentally determined continuous shift of the IR frequency with n and by ab initio calculations^{6,12,28}. Here, we calculated the $^1\text{H-NMR}$ chemical shifts of the protons of water for different cluster number n (Fig. 4a).

The experimentally observed $^1\text{H-NMR}$ chemical shift of 5.25 ppm (Fig. 1c and Supplementary Table S1) is closest to the predicted chemical shift of 5.36 ppm for the cubic octamer D2d structure in Fig. 4b. This assignment does not conflict with the previous experimental and theoretical studies of cubic octamer^{4,5,31}.

The calculation also suggests that the dipole moment of the cubic octamer is zero (Fig. 4a), meaning that the water cluster is a nonpolar entity and differs from “normal” polar water. This helps to explain the long life of the water cluster in hydrophobic solvents. The dipole moment calculation also supports that the observed cluster species is the octamer by excluding polar water clusters with $n = 5-7, 9$, and 10. The suggested cage-like octameric configuration of the water cluster also explains the very low diffusion coefficient of water measured by DOSY spectroscopy, because the diffusivity of the water molecules in the highly ordered water cluster is significantly reduced.

Shields *et al.*⁴ calculated ΔH for formation of an octamer with a static stable hydrogen-bonded structure to be -241 kJ/mol, whereas our experimental value is $\Delta H = -34$ kJ/mol (Fig. 3b). The difference between the two values suggests that the water cluster formed in this study could be composed of dynamic rather than static hydrogen bonding. This agrees with the experimental $^1\text{H-NMR}$ signal with a large chemical shift being observed as a sharp peak rather than split peaks owing to individual protons. Dynamic hydrogen bonding in the size-specific cluster ($n = 8$) is one of the features of the thermodynamically metastable water cluster formed in hydrophobic solvents.

Conventional $^1\text{H-NMR}$ is very effective to investigate the water clusters that easily form in hydrophobic solvents under ambient conditions because of its superior signal resolution to IR and the additional information provided by DOSY, NOESY and relaxation time analysis. A thermodynamic study was performed to characterize the “metastable” state of the water cluster and cluster formation from dissolved water. The dynamic hydrogen bonding in the size-specific cluster is also described, in addition to the nonpolar property of the water cluster. We concluded that water clusters are a cubic octamer, which does not conflict with the previous papers, such as the “square-ice” observed in the hydrophobic conditions recently shown by Algara-Siller, G. *et al.*³².

Water clusters have attracted significant interest in many biological and chemical systems, for example, in bio-inspired materials and devices where water molecules are in contact with or incorporated in organic hydrophobic materials³³⁻³⁹. Investigation of water in organic entities as a matrix by $^1\text{H-NMR}$ is expected to assist formation and stabilization of water clusters and reveal the unique properties of water clusters.

Methods

NMR spectroscopy. One-dimensional and two-dimensional $^1\text{H-NMR}$ spectroscopy were performed with an AVANCE600 spectrometer (Bruker, Yokohama, Japan). The deuterated solvent (0.70 mL), such as benzene- d_6 , was injected into a 5 mm NMR tube and then deionized distilled water was added with a micropipette. The non-deuterated solvents, such as toluene, xylene, and chlorobenzene, were injected into a 5 mm diameter NMR

tube with a 2 mm diameter inner tube containing cyclohexane-d₁₂, which was used as a magnetic field locking system. Tetramethylsilane was used as the internal reference (0.00 ppm). The standard methods of ¹H-NMR, NOESY, and DOSY spectroscopy were used⁴⁰. The NOESY experiments were performed with a 200 ms mixing time. The DOSY experiments were performed under a stimulated echo sequence using bipolar gradients and a longitudinal eddy current delay. A diffusion delay of 40 ms and a gradient pulse length of 3 ms were used to obtain appropriate curves (25 points) for inverse Laplace transformation. The water concentration (mol %) was normalized using saturated dissolved water (0.312 mol %) at 298 K²⁵.

IR spectroscopy. The IR spectra were recorded in transmission mode with a Nicolet 6700 FT-IR spectrometer (ThermoScientific). The samples were kept inside a liquid cell with KBr windows and a polytetrafluoroethylene spacer. For each measurement, the absorption spectrum of benzene-d₆ was subtracted from the measured spectrum.

Theoretical calculations. All of the calculations were performed with the Gaussian 09 program⁴¹. Reported water cluster structures optimized by MP2/CBS-e were used⁴. The theoretical NMR chemical shifts were calculated as the difference of isotropic shielding of the tetramethylsilane at 0.00 ppm. The second-order Møller-Plesset perturbation theory and the gauge-invariant atomic orbital method^{29,30,42} were used combined with the 6-31 + G(d,p) basis set and integral equation formalism for the polarizable continuum model of the benzene solvent.

Reagents. Commercially available deuterated benzene-d₆ (ACROS organics), methanol-d₃, dimethyl sulfoxide-d₆, acetonitrile-d₃, deuterium oxide (Sigma-Aldrich), toluene, xylene, and chlorobenzene (Kanto Kagaku) were used without further purification.

References

- Lupi, L. *et al.* Role of stacking disorder in ice nucleation. *Nature* **551**, 218–222 (2017).
- Brini, E. *et al.* How water's properties are encoded in its molecular structure and energies. *Chem. Rev.* **117**, 12385–12414 (2017).
- Cole, W. T. S., Farrell, J. D., Wales, D. J. & Saykally, R. J. Structure and torsional dynamics of the water octamer from THz laser spectroscopy near 215 nm. *Science* **352**, 1194–1197 (2016).
- Shields, R. M., Temelso, B., Archer, K. A., Morrell, T. E. & Shields, G. C. Accurate predictions of water cluster formation, (H₂O)_n n = 2–10. *J. Phys. Chem. A* **114**, 11725–11737 (2010).
- Gruenloh, C. J. *et al.* Infrared spectrum of a molecular ice cube: The S4 and D(2d) water octamers in benzene-(water)₈. *Science* **276**, 1678–1681 (1997).
- Nauta, K. & Miller, R. E. Formation of cyclic water hexamer in liquid helium: The smallest piece of ice. *Science* **287**, 293–295 (2000).
- Hirabayashi, S. & Yamada, K. M. T. The monocyclic water hexamer detected in neon matrices by infrared spectroscopy. *Chem. Phys. Lett.* **435**, 74–78 (2007).
- Buck, U., Ettischer, I., Melzer, M., Buch, V. & Sadlej, J. Structure and spectra of three-dimensional (H₂O)_n Clusters, n = 8, 9, 10. *Physical Review Letters* **80**(12), 2578–2581 (1998).
- Frank, H. S. & Evans, M. W. Free volume and entropy in condensed systems I. Entropy in binary liquid mixtures; Partial molal entropy in dilute solutions; Structure and thermodynamics in aqueous electrolytes. *J. Chem. Phys.* **13**, 478–492 (1945).
- Frank, H. S. & Evans, M. W. Free volume and entropy in condensed systems III. Entropy in binary liquid mixtures; Partial molal entropy in dilute solutions; Structure and thermodynamics in aqueous electrolytes. *J. Chem. Phys.* **13**, 507–532 (1945).
- Lange, K. M., Hodeck, K. F., Schade, U. & Aziz, E. F. Nature of the hydrogen bond of water in solvents of different polarities. *J. Phys. Chem. B* **114**, 16997–17001 (2010).
- Köddermann, T., Schulte, F., Huelsekopf, M. & Ludwig, R. Formation of water clusters in a hydrophobic solvent. *Angew. Chem. Int. Ed.* **42**, 4904–4908 (2003).
- Scatena, L. F., Brown, M. G. & Richmond, G. L. Water at hydrophobic surfaces: Weak hydrogen bonding and strong orientation effects. *Science* **292**, 908–912 (2001).
- Mallamace, F., Corsaro, C., Mallamace, D., Vasi, S. & Stanley, H. E. NMR spectroscopy study of local correlations in water. *J. Chem. Phys.* **145** (2016).
- Nakahara, M. & Wakai, C. Monomeric and Cluster States of Water Molecules in Organic Solvent. *Chem. Lett.* **21**, 809–812 (1992).
- Easteal, A. J. Tracer Diffusion of Water in Organic Liquids. *J. Chem. Eng. Data* **41**, 741–744 (1996).
- Mammoli, D. *et al.* Challenges in preparing, preserving and detecting parawater in bulk: overcoming proton exchange and other hurdles. *Phys. Chem. Chem. Phys.* **17**, 26819–26827 (2015).
- Chesnut, D. B. Structures, Energies, and NMR Shieldings of Some Small Water Clusters on the Counterpoise Corrected Potential Energy Surface. *J. Phys. Chem. A* **106**, 6876–6879 (2002).
- Chesnut, D. B. & Rusiloski, B. E. A study of NMR chemical shielding in water clusters derived from molecular dynamics simulations. *J. Mol. Struct. THEOCHEM* **314**, 19–30 (1994).
- Mammoli, D. *et al.* Collisional cross-section of water molecules in vapour studied by means of ¹H relaxation in NMR. *Sci. Rep.* **6** (2016).
- Fulmer, G. R. *et al.* NMR chemical shifts of trace impurities: Common laboratory solvents, organics, and gases in deuterated solvents relevant to the organometallic chemist. *Organometallics* **29**, 2176–2179 (2010).
- Holz, M., Heil, S. R. & Sacco, A. Temperature-dependent self-diffusion coefficients of water and six selected molecular liquids for calibration in accurate ¹H NMR PFG measurements. *Phys. Chem. Chem. Phys.* **2**, 4740–4742 (2000).
- Kowert, B. A. Diffusion of benzene and alkylbenzenes in nonpolar solvents. *J. Phys. Chem. B* **122**, 1940–1947 (2018).
- Wakai, C. & Nakahara, M. Attractive potential effect on the self-diffusion coefficients of a solitary water molecule in organic solvents. *J. Chem. Phys.* **106**, 7512–7518 (1997).
- Kirchnerová, J. & Genille, C. B. The solubility of water in low-dielectric solvents. *Can. J. Chem.* **54**(24), 3909–3916 (1976).
- Engineering ToolBox, [online] Available at: <https://www.engineeringtoolbox.com> [Accessed 10 April. 2018] (2001).
- Karlsson, R. Solubility of water in benzene. *J. Chem. Eng. Data* **18**, 290–292 (1973).
- Ludwig, R. Water: From clusters to the bulk. *Angew. Chem. Int. Ed.* **1808**, 40 (2001).
- Gauss, J. Calculation of NMR chemical shifts at second-order many-body perturbation theory using gauge-including atomic orbitals. *Chem. Phys. Lett.* **191**, 614–620 (1992).
- Cancès, E., Mennucci, B. & Tomasi, J. A new integral equation formalism for the polarizable continuum model: Theoretical background and applications to isotropic and anisotropic dielectrics. *J. Chem. Phys.* **107**, 3032–3041 (1997).

31. Slipchenko, L. V. & Gordon, M. S. Water-benzene interactions: An effective fragment potential and correlated quantum chemistry study. *Journal of Physical Chemistry A* **113**(10), 2092–2102 (2009).
32. Algara-Siller, G. *et al.* Square ice in graphene nanocapillaries. *Nature* **519**, 443–445 (2015).
33. Persson, F., Söderhjelm, P. & Halle, B. How proteins modify water dynamics. *J. Chem. Phys.* **148** (2018).
34. Otting, G. & Wüthrich, K. Studies of Protein Hydration in Aqueous Solution by Direct NMR Observation of Individual Protein-Bound Water Molecules. *J. Am. Chem. Soc.* **111**, 1871–1875 (1989).
35. Walia, J. *et al.* Temperature and hydration dependence of proton MAS NMR spectra in MCM-41: Model based on motion induced chemical shift averaging. *Solid State Nucl. Magn. Reson.* **49–50**, 26–32 (2013).
36. Capadona, J. R., Shanmuganathan, K., Tyler, D. J., Rowan, S. J. & Weder, C. Stimuli-responsive polymer Nanocomposites Inspired by the Sea Cucumber Dermis. *Science* **319**, 1370–1374 (2008).
37. Tsubogo, T., Oyamada, H. & Kobayashi, S. Multistep Continuous Flow Synthesis of (R)- and (S)-Rolipram Using Heterogeneous Catalysts. *Nature* **520**, 329–332 (2015).
38. Oka, K., Tsujimura, O., Suga, T., Nishide, H. & Winther-Jensen, B. Light-assisted electrochemical water-splitting at very low bias voltage using metal-free polythiophene as photocathode at high pH in a full-cell setup. *Energy Environ. Sci.* **11**, 1335 (2018).
39. Oyaizu, K. & Nishide, H. Toward flexible batteries. *Science* **319**, 737–738 (2008).
40. Claridge, T. D. W. *High-Resolution NMR Techniques in Organic Chemistry*, Third Edition 1–541 (2016).
41. Frisch, M. J. *et al.* Gaussian 09, Revision D.01 (Gaussian Inc., Wallingford, CT, 2009).
42. Wolinski, K., Hinton, J. F. & Pulay, P. Efficient implementation of the gauge-independent atomic orbital method for NMR chemical shift calculations. *J. Am. Chem. Soc.* **112**, 8251–8260 (1990).

Acknowledgements

This work was partly supported by a Grant-in-Aid for Scientific Research (18H03921), by the Top Global University Project from MEXT, Japan, and the Research Institute for Science and Engineering, Waseda University. K.O. acknowledges support from the Leading Graduate Program in Science and Engineering, Waseda University from MEXT, Japan.

Author Contributions

K.O. and T.S. performed the NMR and IR experiments. K.O., T.S., B.W.-J. and H.N. wrote the paper. N.S. supported the NMR experiments. Y.W. performed the theoretical calculations. H.N. conceived and designed the project.

Additional Information

Supplementary information accompanies this paper at <https://doi.org/10.1038/s41598-018-36787-1>.

Competing Interests: The authors declare no competing interests.

Publisher's note: Springer Nature remains neutral with regard to jurisdictional claims in published maps and institutional affiliations.



Open Access This article is licensed under a Creative Commons Attribution 4.0 International License, which permits use, sharing, adaptation, distribution and reproduction in any medium or format, as long as you give appropriate credit to the original author(s) and the source, provide a link to the Creative Commons license, and indicate if changes were made. The images or other third party material in this article are included in the article's Creative Commons license, unless indicated otherwise in a credit line to the material. If material is not included in the article's Creative Commons license and your intended use is not permitted by statutory regulation or exceeds the permitted use, you will need to obtain permission directly from the copyright holder. To view a copy of this license, visit <http://creativecommons.org/licenses/by/4.0/>.

© The Author(s) 2019